Dalton Transactions

RSC Publishing

PAPER

View Article Online
View Journal | View Issue

Zinc sensors with lower binding affinities for cellular imaging†

Cite this: *Dalton Trans.*, 2013, **42**, 5500

Jin Hoon Kim,[a] In Hong Hwang,[a] Seung Pyo Jang,[a,b] Juhye Kang,[a] Sumi Kim,[c] Insup Noh,[c] Youngmee Kim,[d] Cheal Kim*[a] and Roger G. Harrison*[b]

Received 17th December 2012,
Accepted 10th February 2013

DOI: 10.1039/c3dt33024a

www.rsc.org/dalton

Zinc sensors based on 2,3-dipicolylamine (DPA) and quinoline have been synthesized. They fluoresced in the presence of Zn^{2+} and remained fluorescent when other metal ions were present. Fluorescence enhancement of the sensors was not seen for most other metal ions. *In vitro* studies with fibroblasts showed fluorescence when sensor and Zn^{2+} were present. As seen by single crystal X-ray analysis, four nitrogens from the sensor bind to Zn^{2+}. These new sensors have lower binding constants than the pentadentate sensors based on 2,2-DPA.

Introduction

Biological zinc concentrations range from micromolar to nanomolar. Small molecule sensors have been designed to detect these different cellular levels.[1,2] A large number of the zinc sensors bind strongly and are thus designed to detect zinc at low concentrations, such as the nanomolar region. To help differentiate the different cellular zinc levels, sensors that bind zinc with lower affinities are also important.

Zinc sensors have a zinc-binding domain and fluorophore. The dipicolylamine (DPA) unit is a successful zinc-binding group. In most instances, DPA with pyridyl nitrogens in the 2 positions have been used.[3] The 2,2-DPA group chelates strongly to Zn^{2+} due to it having three nitrogen atoms positioned to bind one zinc ion in a cooperative manner. To modulate the strength of zinc binding, DPA molecules with pyridyl nitrogens in positions 2 and 4 have been synthesized.[4] These sensors have weaker Zn^{2+} binding constants and are useful to image Zn^{2+} in more concentrated pools of biological Zn^{2+}.

A variety of conjugated molecules act as fluorophores for zinc sensors. One of these is quinoline. When an amine is attached to quinoline, its fluorescence is quenched, but bonding by Zn^{2+} to the lone pair on the amine nitrogen promotes fluorescence. Sensors that contain the quinoline group include those with amide amine ethers,[5] hydroxyl quinolines,[6,7] borondipyrromethane,[8] fluorescein[9] and spiropyrans.[10] Quinoline has also been attached to DPA, which has produced sensors with femtomolar zinc detection,[11] large Stokes shifts,[12] fluorescence by two-photon,[13] ratiometric detection,[14] and multiple binding sites.[15]

In this paper, we report the synthesis of two new Zn^{2+} sensors designed to bind Zn^{2+} with weaker affinities than known receptors. They contain 2,3-DPA and quinoline groups. We have measured their fluorescence enhancement in the presence of Zn^{2+} and if they are selective for Zn^{2+} over other metal ions. We have calculated their binding constants and compared them to sensors that have 2,2-DPA subunits. We have also studied these sensors in aqueous solutions and in cells and have found that they can be used to detect Zn^{2+} in both environments.

Results and discussion

The new sensors, **2,3-QA** and **2,3-QP**, were synthesized by adding 2,3-DPA to chloro-quinolineacetamide or 2,3-DPA to chloro-quinolinepropanamide (Scheme 1). The sensors are designed to form a tetradentate binding pocket around Zn^{2+} with all of the chelating atoms being nitrogens. Having one DPA pyridyl nitrogen in the 3 position makes these molecules different form previously reported sensors, which have both pyridyl nitrogens in the 2 positions.[16] The nitrogen in the 3 position is predicted to not bind Zn^{2+} due to it being away from the Zn^{2+} binding domain. The six-membered Zn^{2+} containing chelate ring of **2,3-QP**, predictably, will be less stable than the five-membered ring formed by Zn^{2+} and **2,3-QA**.

[a]*Department of Fine Chemistry, Seoul National University of Science and Technology, Seoul 139-743, Korea. E-mail: chealkim@seoultech.ac.kr*
[b]*Department of Chemistry and Biochemistry, Brigham Young University, Provo, Utah, USA. E-mail: roger_harrison@byu.edu*
[c]*Department of Chemical Engineering, Seoul National University of Science and Technology, Seoul 139-743, Korea*
[d]*Department of Chemistry and Nano Science, Ewha Womans University, Seoul 120-750, Korea*

†Electronic supplementary information (ESI) available: Figures of pH dependence, metal ion inhibition, NMR titrations, Job plots, and cell viability. CCDC 915682. For ESI and crystallographic data in CIF or other electronic format see DOI: 10.1039/c3dt33024a

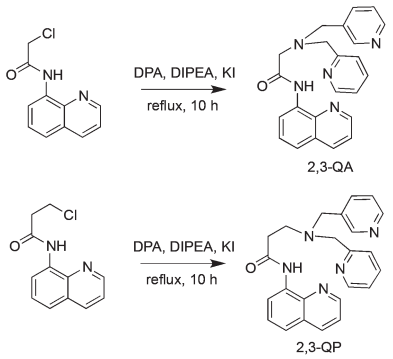

Scheme 1 Synthesis of **2,3-QA** and **2,3-QP**.

Thus, **2,3-QP** is predicted to bind more weakly to Zn^{2+} than **2,3-QA.**

Fluorescence enhancement is observed when Zn^{2+} is added to an aqueous solution of **2,3-QA.** The native fluorescence of **2,3-QA** is minimal, but when Zn^{2+} is added incrementally, fluorescence increases and reaches a maximum at 1 equivalent of Zn^{2+} (Fig. 1). Likewise, when Zn^{2+} is added to **2,3-QP**, fluorescence is enhanced, but doesn't reach a maximum until around 5 equivalents of **2,3-QP.** With **2,3-QA**, the fluorescence maximum is around 510 nm, while with **2,3-QP** it is around 520 nm. The fluorescence enhancement for **2,3-QA** is greater than 200 times that of unbound sensor and for **2,3-QP** it is great than 80 times. This fluorescence enhancement is manifested over a wide pH range. For **2,3-QA**, it lasts from pH = 4 to 10 and for **2,3-QP**, it starts to increase at pH = 4, hits a maximum at around 7 and falls off after 10 (ESI†).

The fluorescence enhancement is selective for Zn^{2+} over other metal ions including Na^{+}, K^{+}, Mg^{2+}, Al^{3+}, Pb^{2+}, Hg^{2+}, Cr^{3+}, Mn^{2+}, Fe^{3+}, Co^{2+}, Ni^{2+}, and Cd^{2+} (Fig. 2). **2,3-QA** shows some response to Cd^{2+}, but the response to Zn^{2+} is over 2 times greater. **2,3-QP** exhibits less of a response to Cd^{2+} and responds to Zn^{2+} 8 times greater than Cd^{2+}. This remarkable selectivity for Zn^{2+} will aid in the detection of it in cells, where other metal ions, such as Na^{+}, K^{+}, and Mg^{2+} are prevalent.

Not only are these sensors selective for Zn^{2+}, their fluorescence due to Zn^{2+} is not inhibited by many other metal ions. When Zn^{2+} and **2,3-QA** are in the presence of one equivalent of other metal ions such as Na^{+}, K^{+}, Mg^{2+}, Al^{3+}, Cr^{3+}, Mn^{2+}, Fe^{3+}, Co^{2+}, Ni^{2+}, Cd^{2+}, Pd^{2+}, and Hg^{2+}, the fluorescence of **2,3-QA** remains strong (Fig. 3). Cu^{2+} does result in some fluorescence reduction. Even with more equivalents of other metal ions,

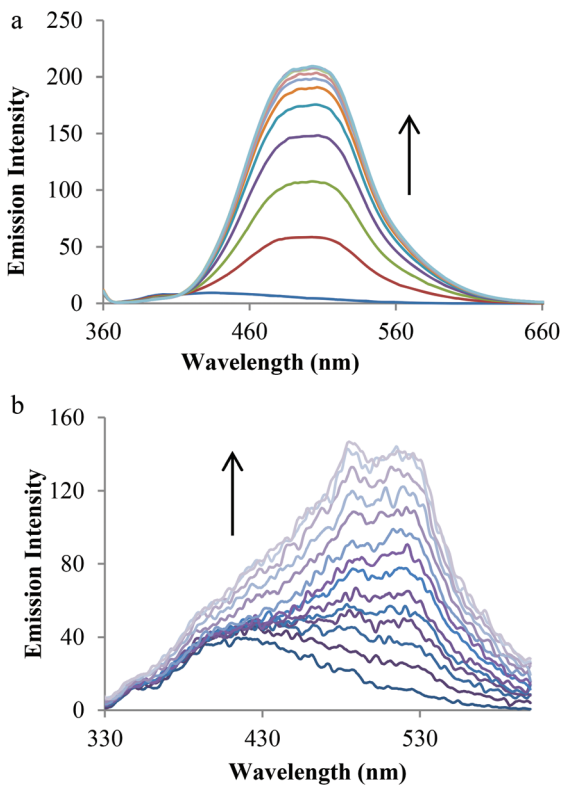

Fig. 1 Fluorescence enhancement of aqueous solutions of **2,3-QA** and **2,3-QP** due to Zn^{2+}. (a) Increase in fluorescence of **2,3-QA** (10 μM) due to 0–1 equivalent of Zn^{2+}. Excited at 350 nm. (b) Increase in fluorescence of **2,3-QP** (10 μM) due to 0–5 equivalents of Zn^{2+}. Excited at 312 nm.

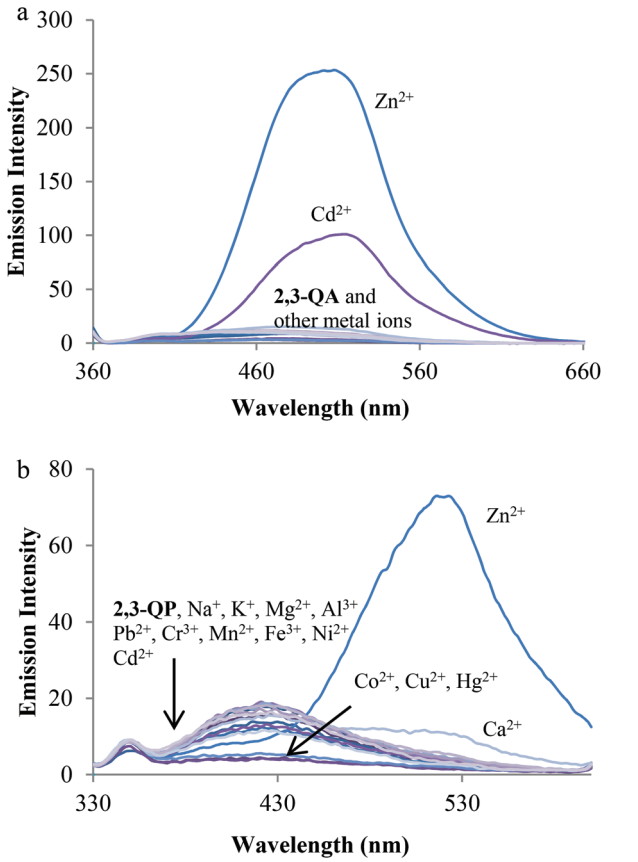

Fig. 2 Fluorescence enhancement of aqueous solutions of **2,3-QA** and **2,3-QP** due to metal ions. (a) Zn^{2+} greatly enhances emission intensity of **2,3-QA** (10 μM), while Cd^{2+} causes some enhancement and other metal ions (Na^{+}, K^{+}, Mg^{2+}, Ca^{2+}, Al^{3+}, Pb^{2+}, Hg^{2+}, Cr^{3+}, Mn^{2+}, Fe^{3+}, Co^{2+}, Ni^{2+}, and Cu^{2+}) cause negligible enhancement. Excitation was at 350 nm. (b) Solutions of **2,3-QP** (5 μM) with 20 equivalents of metal ions excited at 312 nm.

only Co^{2+}, Cu^{2+}, and Hg^{2+} extinguish the fluorescence. The fluorescence of the **2,3-QP**-Zn^{2+} complex is more susceptible to other metal ions. When the same metal ions were in the presence of **2,3-QP** and Zn^{2+}, transition metal ions Mn^{2+}, Fe^{3+}, Co^{2+}, Ni^{2+}, Cu^{2+}, and Hg^{2+} caused fluorescence reduction (ESI†). Thus, Zn^{2+} binds more weakly to **2,3-QP** than it does to **2,3-QA** and other metal ions compete with Zn^{2+} to bind to **2,3-QP.**

These new sensors provide compounds with a wider range of binding constants for Zn^{2+}. The Zn^{2+} dissociation constants for **2,3-QA** and **2,3-QP** were more than 20 times greater than those for the 2,2 analogs (Table 1). Although **2,3-QA** and **2,3-QP** bind Zn^{2+} less strongly, they still have small dissociation constants and will thus be able to bind Zn^{2+} at cellular concentrations. Their Zn^{2+} detection limits are 30 nM for **2,3-QA** and 300 nM for **2,3-QP**. **2,3-QP** has a larger dissociation constant than **2,3-QA**, most likely due to the slightly less favorable six membered metal–ligand ring formation that occurs in the Zn^{2+} complex of **2,3-QP**. The nM dissociation constants are smaller than the K_d's for the weaker binding sensors based on Zinpyr.[4]

To better understand the mode of Zn^{2+} binding, NMR titrations were conducted. As Zn^{2+} was added to **2,3-QA**, the methylene hydrogens of DPA become diastereotopic, split into doublets of doublets, showed geminal coupling, and moved downfield (ESI†). The methylene hydrogens between the DPA amine and amide carbon split as well. Also, the most upfield aromatic hydrogens moved slightly downfield. All of these changes occurred with the addition of one equivalent of Zn^{2+}, implying 1 : 1 binding. The NMR spectra of **2,3-QP** with Zn^{2+} showed broad signals, which were not well defined after one equivalent of Zn^{2+}. To confirm the binding ratio of Zn^{2+}, fluorescence titrations were performed. The fluorescence data were used to make Job plots of **2,3-QA** and **2,3-QP**, which plots show 1 : 1 binding (ESI†).

The crystal structure of the Zn^{2+} complex of **2,3-QA** shows 1 : 1 binding and a distorted square pyramidal geometry around Zn^{2+}. As seen in Fig. 4, a nitrate is at the apex of the pseudo square pyramidal zinc and the nitrogens of **2,3-QA** form the base of the pyramid. The N–Zn–N bond angles are close to 80° (Table 2). Three of the Zn–N bond lengths are close to 2 Å, while the Zn–N bond of the DPA amine nitrogen is longer and 2.24 Å. As predicted, the N from the 3-pyridyl is not coordinated to Zn^{2+}. Also, unlike with some amide containing sensors, the amide N and not the amide O is bonded to Zn^{2+}. The Zn–N_{amide} bond being of similar length to the Zn–$N_{pyridyl}$ bonds, implies that the amide N nitrogen has imine character. This is further supported by the C–O (1.247 Å) and C–N (1.349 Å) amide bond lengths being very close to C–O

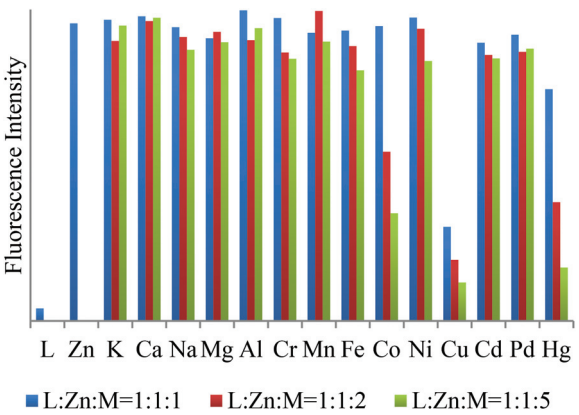

Fig. 3 Fluorescence intensity change when the **2,3-QA**-Zn^{2+} complex is exposed to other metal ions. 10 μM aqueous solutions of **2,3-QA** and Zn^{2+} were exposed to 10, 20, and 50 μM metal ion concentrations. The solutions were excited at 350 nm and the 502 nm emission was monitored.

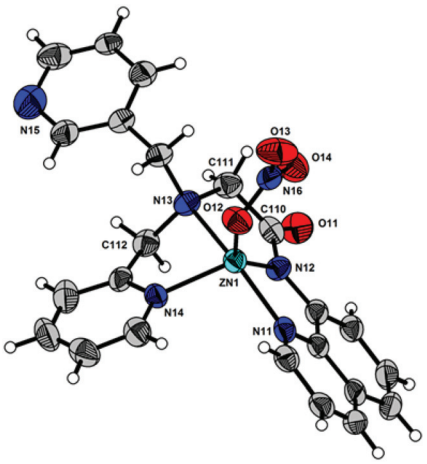

Fig. 4 Crystal structure picture of [**2,3-QA**-$Zn(NO_3)$]NO_3 showing 50% thermal ellipsoids. The outer sphere nitrate is not shown. (Color code: Zn light blue, N blue, O red, C grey, and H white.)

Table 1 UV-vis and fluorescence properties of **QA** and **QP** molecules[a]

	Abs λ/nm (ε unbound)	Abs λ/nm (ε Zn^{2+} bound)	Emission λ/nm (Φ unbound)	Emission λ/nm (Φ Zn^{2+} bound)	Apparent K_d (Zn^{2+})/nM
2,3-QA	305 (4900)	350 (3400)	496 (0.021)	510 (0.107)	0.38
2,2-QA	315 (6100)	355 (4600)	483 (0.002)	515 (0.078)	0.006
2,3-QP	305 (5000)	350 (1500)	425 (0.003)	518 (0.013)	0.53
2,2-QP	315 (6100)	355 (3500)	425 (0.003)	525 (0.057)	0.024

[a] UV-vis of **2,3-QA** and **-QP** with $Zn(NO_3)_2$ was measured in bis-tris buffer (10 mM, water : CH_3OH = 999 : 1 (v/v)) for ε. UV-vis of **2,2′-QA** and **-QP** with $Zn(ClO_4)_2$ was measured in bis-tris buffer (10 mM, water : CH_3CN = 5 : 5 (v/v)) for ε.

(1.22 Å) and C–N (1.33 Å) bond lengths found in common amides. The distorted geometry around Zn^{2+} shows the ability of DPA and Zn^{2+} to conform to different geometries.

Along with characterizing the sensors by NMR and X-ray crystallography, we noted their absorption changes upon Zn^{2+} binding. When Zn^{2+} is added to **2,3-QA** its absorption at 310 nm decreases and a new band at 360 nm grows in (Fig. 5). This new absorption band tails off into the visible, rendering this sensor potentially excitable in the visible light region. **2,3-QP** also has an absorption band at 360 nm that grows in intensity as Zn^{2+} is added to it. As with **2,3-QA**, its band at 310 decreases in intensity as Zn^{2+} is added to it.

After noting the ability of **2,3-QA** to fluoresce in the presence of aqueous Zn^{2+}, we tested it in a cellular environment. Fibroblasts were exposed to 0, 1, 10, and 100 μM Zn^{2+} and then exposed to 10 μM **2,3-QA**. The fibroblasts that were cultured with Zn^{2+} and **2,3-QA** fluoresced (Fig. 6). Those cells cultured without Zn^{2+} or without **2,3-QA** did not fluoresce. The intensity and region of the fluorescence within the cell increased as Zn^{2+} concentration increased. The fluorescence was seen throughout the cell as Zn^{2+} concentrations were increased from 10 to 100 μM, but the middle of the cell, around the nucleus, was the most intense. This new sensor provides a way to image Zn^{2+} in cells.

Control experiments showed fibroblasts survived in the presence of high concentrations (100 μM) of **2,3-QA** (ESI†). When cells were exposed to **2,3-QP** and Zn^{2+} no fluorescence was observed. Most likely, **2,3-QP** is not entering the cells.

Table 2 Selected bond lengths (Å) and angles (°) for the **2,3-QA**-$Zn(NO_3)_2$ complex

Zn(1)–N(11)	2.096(4)	Zn(1)–N(12)	1.998(4)
Zn(1)–N(13)	2.241(4)	Zn(1)–N(14)	2.072(4)
Zn(1)–O(12)	2.026(4)	N(12)–C(110)	1.349(6)
O(11)–C(110)	1.247(6)		
N(12)–Zn(1)–O(12)	141.01(16)	N(12)–Zn(1)–N(14)	119.32(16)
O(12)–Zn(1)–N(14)	99.31(15)	N(12)–Zn(1)–N(11)	80.59(16)
O(12)–Zn(1)–N(11)	98.36(15)	N(14)–Zn(1)–N(11)	100.65(15)
N(12)–Zn(1)–N(13)	79.11(15)	O(12)–Zn(1)–N(13)	104.83(15)
N(14)–Zn(1)–N(13)	79.39(16)	N(11)–Zn(1)–N(13)	156.53(15)

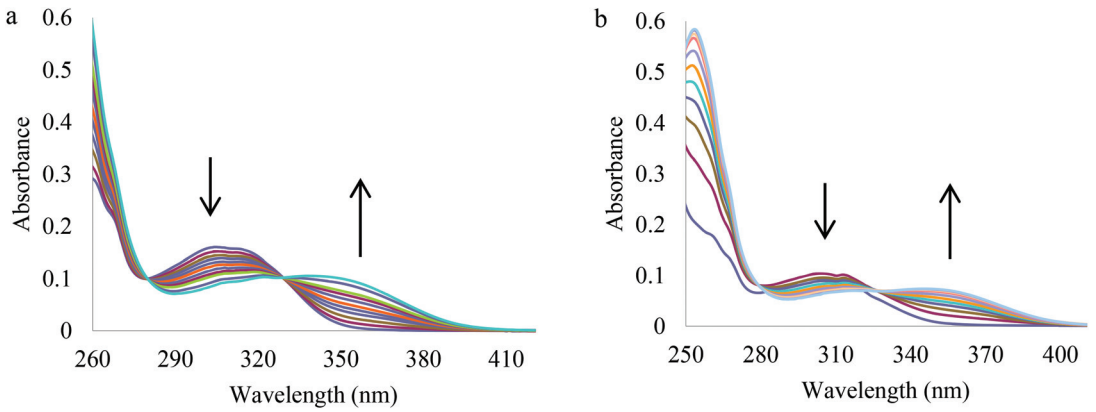

Fig. 5 Absorption change of **2,3-QA** and **2,3-QP** due to Zn^{2+} addition. Zero to 3 equivalents of Zn^{2+} were added to 20 μM aqueous solutions of (a) **2,3-QA** and (b) **2,3-QP**.

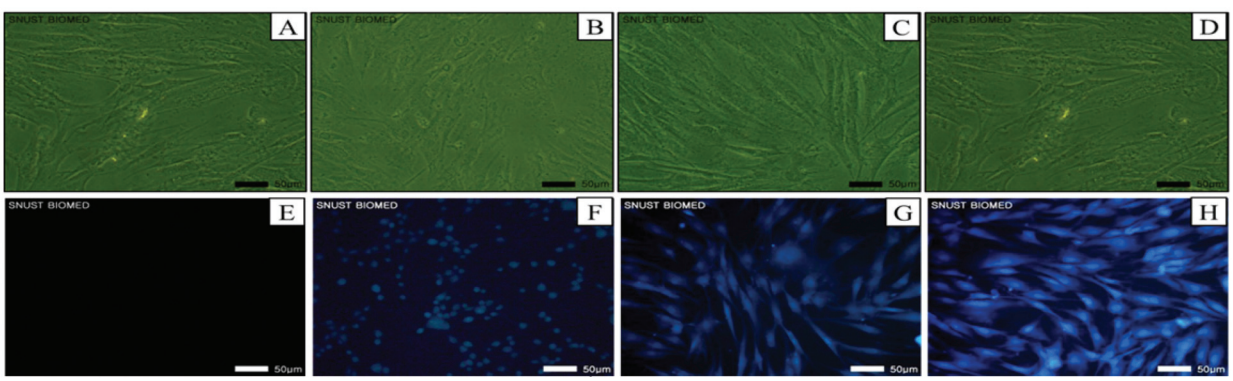

Fig. 6 Fluorescence images of fibroblasts cultured with Zn^{2+} and **2,3-QA**. Cells were exposed to 0 (A and E), 1 (B and F), 10 (C and G), and 100 (D and H) μM $Zn(NO_3)_2$ for four hours and then later with 10 μM **2,3-QA** for 30 min. The top images (A–D) were observed with the light microscope and the bottom images were taken with a fluorescence microscope. The scale bar is 50 μm.

Conclusions

Sensors containing 2,3-DPA and quinoline have been synthesized. Their fluorescence is greatly enhanced when bound to Zn^{2+} and they are selective for Zn^{2+} over other metal ions. A crystal structure of **2,3-QA** with Zn^{2+} shows four Zn–N bonds and one nitrate–Zn bond. With one pyridine of DPA not coordinated to Zn^{2+}, these sensors have weaker Zn^{2+} binding constants than the 2,2-DPA Zn^{2+} sensors. The **2,3-QA** sensor is useful in detecting Zn^{2+} in fibroblasts.

Experimental section

Materials and instruments

All the solvents and reagents were obtained from Sigma-Aldrich and used as received. 3-Chloro-*N*-(quinolin-8-yl)propanamide and 2-chloro-*N*-(naphthalen-4-yl)acetamide were synthesized as previous reported.[16] Absorption spectra were recorded at 25 °C using a Perkin Elmer model Lambda 2S UV/Vis spectrometer. Fluorescence measurements were performed on a Perkin Elmer model LS45 fluorescence spectrometer. X-ray diffraction data were collected on a Bruker SMART AXS diffractometer. ^{1}H NMR and ^{13}C NMR measurements were performed on a Varian 400 MHz spectrometer and chemical shifts are recorded in ppm. Electrospray ionization mass spectra (ESI-MS) were acquired on a hybrid ion-trap time-of-flight mass spectrometer (Shimadzu LCMS-IT-TOF, Kyoto, Japan) equipped with an ESI source (ESI-IT-TOFMS). Elemental analysis for carbon, nitrogen, and hydrogen was carried out using a Flash EA 1112 elemental analyzer (thermo) at the Organic Chemistry Research Center of Sogang University, Korea.

Synthesis

Synthesis of 2,3-DPA: 2,3-DPA was prepared by a modified literature procedure.[17] A solution of 3-(aminomethyl)pyridine (0.52 mL, 5.1 mmol) and 2-pyridylcarboxaldehyde (0.48 mL, 5 mmol) in 10 mL of MeOH was stirred for 5 min. $NaBH_4$ (0.21 g, 5.5 mmol) was then added slowly over 5 min. The resulting red solution was stirred overnight, followed by addition of 10 drops of concentrated HCl. The solution was concentrated to afford a red oil and then diluted with 50 mL of H_2O. Extraction with $CHCl_3$, washing with saturated aqueous $NaHCO_3$, drying over Na_2SO_4, and evaporating the solvent yielded an amber oil. The pure product was obtained by column chromatography (silica gel, chloroform–methanol 10 : 1). Yield: 0.52 g (52.2%). ^{1}H NMR (400 MHz, DMSO-d_6, 25 °C): δ = 8.53 (s, 1H), 8.48 (d, 1H), 8.43 (d, 1H), 7.74 (m, 2H), 7.45 (d, 1H), 7.33 (t, 1H), 7.23 (t, 1H) 3.78 (s, 2H), 3.73 (s, 2H), 2.86 (s, 1H) ppm. The mass spectrum matched the literature value.

Synthesis of **2,3-QA**: 2-chloro-*N*-(quinolin-8-yl)acetamide (0.46 g, 2.1 mmol), 2,3-DPA (0.40 g, 2 mmol), *N*,*N*-diisopropylethylamine (0.39 mL, 2.2 mmol) and potassium iodide (0.37 g, 2.2 mmol) were dissolved in acetonitrile (30 mL), stirred and refluxed for 1 day at 60 °C. The solution was extracted 3 times with dichloromethane. The organic phase was separated, the solvent was removed *in vacuo* and the pure product was obtained by column chromatography (silica gel, chloroform–methanol (30 : 1, v/v)). Yield: 0.35 g (46.1%). ^{1}H NMR (400 MHz, DMSO-d_6, 25 °C): δ = 11.44 (s, 1H), 9.10 (d, 1H), 8.78 (s, 1H), 8.61 (d, 1H), 8.49 (d, 1H), 8.44 (m, 2H), 8.07 (d, 1H), 7.81 (m, 2H), 7.71 (m, 2H), 7.57 (t, 1H), 7.35 (t, 1H), 7.25 (t, 1H), 3.89 (s, 2H), 3.84 (s, 2H), 3.46 (s, 2H) ppm. ^{13}C NMR (400 MHz, DMSO-d_6, 25 °C): δ = 168.9, 157.8, 150.4, 149.1, 149.0, 148.7, 137.8, 136.8, 136.7, 133.9, 133.3, 127.8, 127.1, 123.5, 123.2, 122.6, 122.4, 121.8, 115.3, 59.8, 55.9 ppm. HRMS (ESI): *m*/*z* calcd for $C_{23}H_{21}N_5O + H^+$: 384.18 [M + H^+]: found, 384.18. Elemental analysis calcd (%) for $C_{23}H_{21}N_5O$ (383.45): C 72.04, H 5.52, N 18.26; found: C 71.73, H 5.36, N 18.16.

Synthesis of **2,3-QP**: 2-chloro-*N*-(quinolin-8-yl)propanamide (0.49 g, 2.1 mmol), 2,3-DPA (0.40 g, 2 mmol), *N*,*N*-diisopropylethylamine (0.39 mL, 2.2 mmol) and potassium iodide (0.37 g, 2.2 mmol) were dissolved in acetonitrile (30 mL), stirred and refluxed for 1 day at 60 °C. The solution was extracted 3 times with dichloromethane. The organic phase was separated, the solvent was removed *in vacuo* and the pure product was obtained by column chromatography (silica gel, chloroform–methanol (30 : 1, v/v)). Yield: 0.34 g (43.0%). ^{1}H NMR (400 MHz, DMSO-d_6, 25 °C): δ = 10.58 (s, 1H), 8.87 (d, 1H), 8.67 (d, 1H), 8.61 (s, 1H), 8.45 (d, 1H), 8.41 (m, 2H), 7.80 (d, 1H), 7.67 (m, 5H), 7.21 (m, 2H), 3.78 (d, 4H), 2.86 (m, 4H). ^{13}C NMR (400 MHz, DMSO-d_6, 25 °C): δ = 170.9, 158.8, 150.2, 148.7, 148.7, 148.2, 136.6, 136.6, 136.3, 134.9, 134.0, 127.9, 127.0, 123.2, 122.9, 122.1, 121.7, 116.7, 58.8, 54.5, 50.0, 34.9 ppm. HRMS (ESI): *m*/*z* calcd for $C_{24}H_{23}N_5O + H^+$: 398.20 [M + H^+]; found, 398.19. Elemental analysis calcd (%) for $C_{24}H_{23}N_5O$ (397.47): C 72.52, H 5.83, N 17.62; found: C 72.48, H 5.78, N 17.68.

Crystallization of **2,3-QA**-$Zn(NO_3)_2$: A methanol solution of $Zn(NO_3)_2$ (14.6 mg, 0.05 mmol, 1 mL) was added dropwise to a methanol solution of **2,3-QA** (38.3 mg, 0.1 mmol, 1 mL). Colorless crystals of **2,3-QA**-$Zn(NO_3)_2$ were obtained after 1 day.

The diffraction data for the complex was collected on a Bruker SMART AXS diffractometer using Mo Kα (λ = 0.71073 Å). The crystal was mounted on a glass fiber under epoxy. The CCD data were integrated and scaled using a Bruker SAINT, and the structures were solved and refined using SHELXTL. Hydrogen atoms were located in the calculated positions. Crystallographic data for **2,3-QA**-$Zn(NO_3)_2$: $C_{48.50}H_{48}N_{14}O_{16.50}Zn_2$, M = 1221.75, monoclinic, space group $P2_1/c$, a = 12.458(3) Å, b = 33.214(7) Å, c = 13.177(3) Å, α = 90.00°, β = 97.57(3)°, γ = 90.00°, V = 5404.9(19) Å^3, room temperature, Z = 4, μ = 0.971 mm^{-1}, ρ_c = 1.501 g cm^{-3}, crystal size 0.40 × 0.28 × 0.05 mm^3, 29 974 reflections collected with 10 545 being independent (R_{int} = 0.0432); the final R_1 and wR (F^2) values were 0.0709 [$I > 2\sigma(I)$] and 0.2038, respectively; data completeness to θ = 26.00° 99.3%; goodness-of-fit on F^2 = 1.045. The CIF deposition number is CCDC-915682.

Optical measurements

UV-vis: sensors (38.3 mg, 0.1 mmol for **2,3-QA** and 39.7 mg, 0.1 mmol for **2,3-QP**) were dissolved in methanol (5 mL) and

3 μL of each (20 mM) was diluted to 2.997 mL with bis-tris buffer (10 mM) to make a final concentration of 20 μM. $Zn(NO_3)_2$ (30.0 mg, 0.1 mmol) was dissolved in methanol (5 mL) and 0.3–9 μL of metal solution (20 mM) was transferred to each sensor solution (20 μM). After mixing, UV absorption spectra were taken at room temperature.

Fluorescence: bis-tris (4.184 g, 0.10 mol) was dissolved in water (200 mL) and 0.2 mL of 30% HCl was added to it to adjust the pH to 7. **2,3-QA** (38.3 mg, 0.10 mmol) was dissolved in methanol (10 mL) and 3 μL of this 10 mM solution was diluted with 2.997 mL of bis-tris buffer (10 mM) to make the final concentration of 10 μM. $Zn(NO_3)_2$ (30.0 mg, 0.10 mmol) was dissolved in methanol (5 mL) and quantities of this Zn^{2+} solution (20 mM) were transferred to each sensor solution (10 μM) to give 1–20 equivalents. After mixing, fluorescence spectra were taken at room temperature.

2,3-QP (19.9 mg, 0.05 mmol) was dissolved in methanol (10 mL) and 3 μL of this solution (5 mM) was diluted with 2.997 mL bis-tris buffer (10 mM) to make a final concentration of 5 μM. $Zn(NO_3)_2$ (30.0 mg, 0.1 mmol) was dissolved in methanol (5 mL) and some solution (20 mM) was transferred to each **2,3-QP** solution (5 μM) to make 1–20 equivalent solutions. After mixing, fluorescence spectra were taken at room temperature.

Competition with other metal ions: **2,3-QA** (38.3 mg, 0.10 mmol) was dissolved in methanol (10 mL) and 3 μL of the solution (10 mM) was diluted with 2.997 mL bis-tris buffer (10 mM) to make a final concentration of 10 μM. Solutions of 5 μM **2,3-QA** were prepared in the same way. MNO_3 (M = Na, K, Ag, 0.1 mmol) or $M(NO_3)_2$ (M = Mn, Fe, Co, Ni, Cu, Zn, Cd, Mg, Ca, Pb, Hg, 0.1 mmol) or $M(NO_3)_3$ (M = Al, 0.1 mmol) were dissolved in methanol (10 mL). 3 μL of each metal solution (10 mM) were taken and added to 3 mL of **2,3-QA** solution (10 μM) to give 1 equivalent of metal ion. After mixing, fluorescence spectra were taken at room temperature. Then, 3 μL of Zn^{2+} solution (10 mM) was added into the mixed solution of each metal ion and **2,3-QA** to make 1 equivalent. After mixing, fluorescence spectra were taken at room temperature.

2,3-QP (19.9 mg, 0.05 mmol) was dissolved in methanol (10 mL) and 3 μL of this solution (5 mM) was diluted with 2.997 mL of bis-tris buffer (10 mM) to make a final concentration of 5 μM. MNO_3 (M = Na, K, Ag, 0.5 mmol) or $M(NO_3)_2$ (M = Mn, Fe, Co, Ni, Cu, Zn, Cd, Mg, Ca, Pb, Hg, 0.5 mmol) or $M(NO_3)_3$ (M = Al, 0.5 mmol) were dissolved in methanol (10 mL). 3 μL of each metal solution (50 mM) was taken and added into 3 mL of **2,3-QP** solution (5 μM) to give 10 equivalent solutions. After mixing, fluorescence spectra were taken at room temperature. Then, 3 μL of Zn^{2+} solution (50 mM) was added into the mixed solution of each metal ion and **2,3-QP** to give 10 equivalents of Zn^{2+}. After mixing, fluorescence spectra were taken at room temperature.

Job plot measurements: **2,3-QA** (38.3 mg, 0.10 mmol) was dissolved in methanol (10 mL). Volumes 12, 10.8, 9.6, 8.4, 7.2, 6.0, 4.8, 3.6, 2.4, and 1.2 μL of the **2,3-QA** solution were taken and transferred to vials. Each vial was diluted with bis-tris buffer (10 mM) to make a total volume of 2.988 mL. $Zn(NO_3)_2$ (30.0 mg, 0.10 mmol) was dissolved in methanol (10 mL). Volumes of 0, 1.2, 2.4, 3.6, 4.8, 6.0, 7.2, 8.4, 9.6, 10.8, and 12 μL of the $Zn(NO_3)_2$ solution were added to each diluted **2,3-QA** solution. Each vial had a total volume of 3 mL. After shaking, UV-vis and fluorescence were taken at room temperature.

2,3-QP (79.4 mg, 0.20 mmol) was dissolved in methanol (10 mL). Volumes of 12, 10.8, 9.6, 8.4, 7.2, 6.0, 4.8, 3.6, 2.4, and 1.2 μL of **2,3-QP** solution were taken and transferred to vials. Each vial was diluted with bis-tris buffer (10 mM) to make a total volume of 2.988 mL. $Zn(NO_3)_2$ (60.0 mg, 0.2 mmol) was dissolved in methanol (10 mL). Volumes of 0, 1.2, 2.4, 3.6, 4.8, 6.0, 7.2, 8.4, 9.6, 10.8, and 12 μL of the $Zn(NO_3)_2$ solution were added to each diluted **2,3-QP** solution. Each vial had a total volume of 3 mL. After shaking, UV-vis and fluorescence were taken at room temperature.

Quantum yield measurements: **2,3-QA** (38.3 mg, 0.10 mmol) and $Zn(NO_3)_2$ (30.0 mg, 0.10 mmol) were dissolved in methanol (10 mL). Quinine hemisulfate monohydrate (21.7 mg, 0.05 mmol) was dissolved in 0.1 M H_2SO_4 (10 mL). UV-vis spectra of **2,3-QA** (20 μM) were taken with and without $Zn(NO_3)_2$ (20 μM) in bis-tris buffer (10 mM). UV-vis spectra of quinine hemisulfate monohydrate (5, 10, 15, 20, 25 μM) were taken in 0.1 M H_2SO_4 solution. Fluorescence spectra of **2,3-QA** (20 μM) were taken with and without $Zn(NO_3)_2$ (20 μM) in bis-tris buffer (10 mM) after excited at 350 nm. Fluorescence spectra of quinine hemisulfate monohydrate (2.3, 19.2 μM) were taken in 0.1 M H_2SO_4 solution after excited at 350 nm (Φ = 0.107). Quantum yield was adjusted according to UV-vis absorption intensities.

2,3-QP (39.7 mg, 0.10 mmol) and $Zn(NO_3)_2$ (30.0 mg, 0.10 mmol) were dissolved in methanol (10 mL). Quinine hemisulfate monohydrate (21.7 mg, 0.05 mmol) was dissolved in 0.1 M H_2SO_4 (10 mL). UV-vis spectra of **2,3-QP** (20 μM) were taken with and without $Zn(NO_3)_2$ (20 μM) in bis-tris buffer (10 mM) and UV-vis of quinine hemisulfate monohydrate (5, 10, 15, 20, 25 μM) were taken in 0.1 M H_2SO_4 solution. Fluorescence spectra of **2,3-QP** (20 μM) were taken with and without $Zn(NO_3)_2$ (20 μM) in bis-tris buffer after excited at 312 nm. Fluorescence spectra of quinine hemisulfate monohydrate (15.4, 25.7 μM) were taken in 0.1 M H_2SO_4 solution excited at 312 nm (Φ = 0.013). Quantum yield was adjusted according to UV-vis absorption intensities.

Equilibrium constants: to calculate the equilibrium constant for **2,3-QA**-Zn^{2+} and **2,3-QP**-Zn^{2+}, the method of Nagano *et al*. was used, which entailed adding the sensors to a HEPES buffer solution of Zn^{2+} and nitrilotriacetic acid.[18] Fluorescence changes were monitored under these conditions and used to calculate apparent dissociation constants.

NMR titrations

For ^1H NMR titrations of **2,3-QA**, five NMR tubes of **2,3-QA** (38.3 mg, 0.10 mmol) dissolved in DMSO-d_6 (50 μL) were prepared, and five different concentrations (0.02, 0.04, 0.06, 0.08 and 0.10 mmol) of $Zn(NO_3)_2$ dissolved in CD_3CN (0.95 mL)

were added to each solution of **2,3-QA**. After shaking, NMR spectra were taken.

For ^{1}H NMR titrations of **2,3-QP**, five NMR tubes of **2,3-QP** (39.7 mg, 0.10 mmol) dissolved in CD_3CN (0.5 mL) were prepared, and five different concentrations (0.02, 0.04, 0.06, 0.08 and 0.10 mmol) of $Zn(NO_3)_2$ dissolved in CD_3CN (0.5 mL) were added to each solution of **2,3-QP**. After shaking, NMR spectra were taken.

Methods for cell imaging

Human dermal fibroblast cells in low passage were cultured in FGM-2 medium (Lonza, Switzerland) supplemented with 10% fetal bovine serum, 1% penicillin/streptomycin in the *in vitro* incubator with 5% CO_2 at 37 °C. Cells were seeded onto a 12 well plate (SPL Lifesciences, Korea) at a density of 2×10^5 cells per well and then incubated at 37 °C for 4 h after additions of various concentrations (0–100 μM) of $Zn(NO_3)_2$. After washing with phosphate buffered saline (PBS) three times to remove the remaining $Zn(NO_3)_2$, the cells were incubated with 10 μM **2,3-QA** at room temperature for 30 min. Subsequent to washing of the incubated cells with PBS, the cells were observed by using a microscope (Olympus, Japan). The fluorescent images of the cells were obtained by using a fluorescence microscope (Leica DMLB, Germany) at the excitation wavelength of 515–560 nm.

Fluorescence visualization of the cell viability previously exposed to the $Zn(NO_3)_2$ was performed with the live and dead viability/cytotoxicity kit for mammalian cells (Invitrogen, USA). After *in vitro* incubation and exposure to the $Zn(NO_3)_2$, a live and dead viability/cytotoxicity assay was prepared by adding 1.2 μL ethidium homodimer-1 (EthD-1) solution (2 mM) and 4 mM calcein AM solution (0.3 μL) into 600 μL PBS. After letting the cells react with the prepared assay solution for 30 min in the *in vitro* incubator, cell viability was observed by a fluorescence microscope (Leica DMLB, Germany), where the live cells were observed to be blue and the dead ones as red.

Acknowledgements

Financial support from Converging Research Center Program through the National Research Foundation of Korea (NRF) funded by the Ministry of Education, Science and Technology (2012001725 and 2012008875), and Brigham Young University is gratefully acknowledged.

Notes and references

1 N. C. Lim, H. C. Freake and C. Brückner, *Chem.–Eur. J.*, 2005, **11**, 38; Z. Dai and J. W. Canary, *New J. Chem.*, 2007, **31**, 1708; E. L. Que, W. Eomaille and C. J. Chang, *Chem. Rev.*, 2008, **108**, 1517; E. Tomat and S. J. Lippard, *Curr. Opin. Chem. Biol.*, 2010, **14**, 225.

2 L. E. McQuade and S. J. Lippard, *Inorg. Chem.*, 2010, **49**, 9535; B. A. Smith, W. J. Akers, W. M. Leevy, A. J. Lampkins, S. Xiao, W. Wolter, M. A. Suckow, S. Achilefu and B. D. Smith, *J. Am. Chem. Soc.*, 2010, **132**, 67; Z. Xu, K.-H. Baek, H. N. Kim, J. Cui, X. Qian, D. R. Spring, I. Shin and J. Yoon, *J. Am. Chem. Soc.*, 2010, **132**, 601; E. M. Nolan and S. J. Lippard, *Acc. Chem. Res.*, 2009, **42**, 193; Y. Mei, C. J. Frederickson, L. J. Giblin, J. H. Weiss, Y. Medvedeva and P. A. Bentley, *Chem. Commun.*, 2011, **47**, 7107.

3 Recent examples: J. Meeusen, H. Tomasiewicz, A. Nowakowski and D. H. Petering, *Inorg. Chem.*, 2011, **50**, 7563; X.-B. Yang, B.-X. Yang, J.-F. Ge, Y.-J. Xu, Q.-F. Xu, J. Liang and J.-M. Lu, *Org. Lett.*, 2011, **13**, 2710; P. Das, S. Bhattacharya, S. Mishra and A. Das, *Chem. Commun.*, 2011, **47**, 8118; A. E. Lee, M. R. Grace, A. G. Meyer and K. L. Tuck, *Tetrahedron Lett.*, 2010, **51**, 1161; Z. Liu, C. Zhang, Y. Li, Z. Wu, F. Qian, X. Yang, W. He, X. Gao and Z. Guo, *Org. Lett.*, 2009, **11**, 795; J. E. Kwon, S. Lee, Y. You, K.-H. Baek, K. Ohkubo, J. Cho, S. Fukuzumi, I. Shin, S. Y. Park and W. Nam, *Inorg. Chem.*, 2012, **51**, 8760; H. G. Lee, J. H. Lee, S. P. Jang, H. M. Park, S.-J. Kim, Y. Kim, C. Kim and R. G. Harrison, *Tetrahedron*, 2011, **67**, 8073; G.-C. Kuang, J. R. Allen, M. A. Baird, B. T. Nguyen, L. Zhang, T. J. Morgan Jr., C. W. Levenson, M. W. Davidson and L. Zhu, *Inorg. Chem.*, 2011, **50**, 10493; J. F. Zhang, S. Kim, J. H. Han, S.-J. Lee, T. Pradhan, Q. Y. Cao, S. J. Lee, C. Kang and J. S. Kim, *Org. Lett.*, 2011, **13**, 5294; L. Xue, G. Li, C. Yu and H. Jiang, *Chem.–Eur. J.*, 2012, **18**, 1050; X. Wang, Z. Liu, F. Qian and W. He, *Inorg. Chem. Commun.*, 2012, **15**, 176; X. Meng, S. Wang, Y. Li, M. Zhu and Q. Guo, *Chem. Commun.*, 2012, **48**, 4196; Z. Xu, G.-H. Kim, S. J. Han, M. J. Jou, C. Lee, I. Shin and J. Yoon, *Tetrahedron*, 2009, **65**, 2307; K. Hanaoka, Y. Muramatsu, Y. Urano, T. Terai and T. Nagano, *Chem.–Eur. J.*, 2010, **16**, 568; S. Atilgan, T. Ozdemir and E. U. Akkaya, *Org. Lett.*, 2008, **10**, 4065; W. Jiang, Q. Fu, H. Fan and W. Wang, *Chem. Commun.*, 2008, 259; F. Qian, C. Zhang, Y. Zhang, W. He, X. Gao, P. Hu and Z. Guo, *J. Am. Chem. Soc.*, 2009, **131**, 1460.

4 B. A. Wong, S. Friedle and S. J. Lippard, *Inorg. Chem.*, 2009, **48**, 7009.

5 Y. Zhang, X. Guo, L. Jia, S. Zu, Z. Xu, L. Zheng and X. Qian, *Dalton Trans.*, 2012, **41**, 11776; Y. Zhang, X. Guo, W. Si, L. Jia and X. Qian, *Org. Lett.*, 2008, **10**, 473.

6 X. Zhou, B. Yu, Y. Guo, X. Tang, H. Zhang and W. Liu, *Inorg. Chem.*, 2010, **49**, 4002; X. Zhou, P. Li, Z. Shi, X. Tang, C. Chen and W. Liu, *Inorg. Chem.*, 2012, **51**, 9226; R.-M. Wang, S.-B. Huang, N. Zhao and Z.-N. Chen, *Inorg. Chem. Commun.*, 2010, **13**, 1432.

7 C. Núñez, R. Bastida, A. Macías, E. Bértolo, L. Fernandes, J. L. Capelo and C. Lodeiro, *Tetrahedron*, 2009, **65**, 6179; M. Mameli, M. C. Aragoni, M. Arca, M. Atzori, A. Bencini, C. Bazzicalupi, A. J. Blake, C. Caltagirone, F. A. Devillanova, A. Garau, M. B. Hursthouse, F. Isaia, V. Lippolis and B. Valtancoli, *Inorg. Chem.*, 2009, **48**, 9236; J. Jiang, T. Xiaoliang, L. Yang, W. Dou, W. Liu, R. Fang and W. Liu, *Dalton Trans.*, 2011, **40**, 6367; I. Ravikumar and P. Ghosh, *Inorg. Chem.*, 2011, **50**, 4229.

8 C. Zhao, Y. Zhang, P. Feng and J. Cao, *Dalton Trans.*, 2012, **41**, 831.
9 E. M. Nolan, J. Jaworski, K.-I. Okamoto, Y. Hayashi, M. Sheng and S. J. Lippard, *J. Am. Chem. Soc.*, 2005, **127**, 16812.
10 J.-F. Zhu, H. Yuan, W.-H. Chan and A. W. M. Lee, *Tetrahedron Lett.*, 2010, **51**, 3550.
11 H.-H. Wang, Q. Gan, X.-J. Wang, L. Xue, S.-H. Liu and H. Jiang, *Org. Lett.*, 2007, **9**, 4995.
12 L. Xue, C. Liu and H. Jiang, *Chem. Commun.*, 2009, 1061.
13 X.-Y. Chen, J. Shi, Y.-M. Li, F. L. Wang, X. Wu, Q. X. Guo and L. Liu, *Org. Lett.*, 2009, **11**, 4426.
14 L. Xue, Q. Liu and H. Jiang, *Org. Lett.*, 2009, **11**, 3454; Z. Liu, C. Zhang, Y. Li, Z. Wu, F. Qian, X. Yang, W. He, X. Gao and Z. Guo, *Org. Lett.*, 2009, **11**, 795; E. Tomat and S. J. Lippard, *Inorg. Chem.*, 2010, **49**, 9113; Z. Xu, K.-H. Baek, H. N. Kim, J. Cui, X. Qian, D. R. Spring, I. Shin and J. Yoon, *J. Am. Chem. Soc.*, 2010, **132**, 601.
15 Y. Mikata, A. Yamashita, K. Kawata, H. Konno, S. Itami, K. Yasuda and S. Tamotsu, *Dalton Trans.*, 2011, **40**, 4059.
16 H. G. Lee, J. H. Lee, S. P. Jang, I. H. Hwang, S.-J. Kim, J. Kim, C. Kim and R. G. Harrison, *Inorg. Chim. Acta*, 2013, **394**, 542.
17 M. Soibinet, I. Déchamps-Olivier, A. Mohamadou and M. Aplincourt, *Inorg. Chem. Commun.*, 2004, **7**, 405.
18 S. Maruyama, K. Kikuchi, T. Hirano, Y. Urano and T. Nagano, *J. Am. Chem. Soc.*, 2002, **124**, 10650.